Article:
Feingold, G, McComiskey, A, Yamaguchi, T et al. (3 more authors) (2016) New Approaches to Quantifying Aerosol Influence on the Cloud Radiative Effect. Proceedings of the National Academy of Sciences, 113 (21). pp. 5812-5819. ISSN 1091-6490

https://doi.org/10.1073/pnas.1514035112

New Approaches to Quantifying Aerosol Influence on the Cloud Radiative Effect

G. Feingold[a], A. McComiskey[b], T. Yamaguchi[a,c], J. S. Johnson[d], K. S. Carslaw[d] and K. S. Schmidt[e]

In Press

[a] NOAA Earth System Research Laboratory, Chemical Sciences Division, Boulder, Colorado
graham.feingold@noaa.gov

[b] NOAA Earth System Research Laboratory, Global Monitoring Division, Boulder, Colorado

[c] Cooperative Institute for Research in Environmental Sciences (CIRES), University of Colorado, Boulder

[d] Institute for Climate and Atmospheric Science, School of Earth and Environment, University of Leeds, Leeds, United Kingdom

[e] Laboratory for Atmospheric and Space Physics (LASP), University of Colorado, Boulder

Abstract

The topic of cloud radiative forcing associated with the atmospheric aerosol has been the focus of intense scrutiny for decades. The enormity of the problem is reflected in the need to understand aspects such as aerosol composition, optical properties, cloud condensation and ice nucleation potential, along with the global distribution of these properties, controlled by emissions, transport, transformation, and sinks. Equally daunting is that clouds themselves are complex, turbulent, microphysical entities, and by their very nature, ephemeral and hard to predict. Atmospheric general circulation models represent aerosol-cloud interactions at ever-increasing levels of detail but these models lack the resolution to represent clouds and aerosol-cloud interactions adequately. There is a dearth

of observational constraints on aerosol-cloud interactions. We develop a conceptual approach to systematically constrain the aerosol-cloud radiative effect in shallow clouds through a combination of routine process modeling, and satellite and surface-based shortwave radiation measurements. We heed the call to merge Darwinian and Newtonian strategies by balancing microphysical detail with scaling and emergent properties of the aerosol-cloud-radiation system.

\body

Introduction

The climate system, with its couplings between land surface, vegetation, ocean, cryosphere, and atmosphere, is an extraordinarily complex system that is under intensive scrutiny for the purposes of climate analysis and prediction. The atmospheric aerosol and its interaction with clouds is a poorly quantified component of the climate system and is the focus of the current study. The aerosol comprises suspended particles that derive from the oceans, land surface, volcanoes, and anthropogenic activities. The difficulty in quantifying climate forcing by the aerosol emanates partly from the complexity in the aerosol itself, and partly from the fact that its influence on clouds requires detailed understanding of clouds and cloud feedbacks at a range of spatiotemporal scales. Untangling the multiple cloud responses that occur as a result of aerosol perturbations is particularly difficult (1). As one example, consider the influence of the aerosol on clouds and precipitation. Assuming no change in condensed water, the aerosol, by acting as nucleation sites for droplets, might generate smaller droplets, more reflective clouds (2), and reduced precipitation (3). But through a multitude of complex and contingent pathways, aerosol-perturbed clouds sometimes appear to have similar reflectance because

brightening is offset by reductions in cloud water, a fundamental property controlling cloud reflectance. On short timescales (hours), the aerosol tends to reduce precipitation in shallow, liquid-only clouds but this may be offset over longer periods (multiple days) (4). Deep, mixed-phase convective clouds present even more complex pathways for generation of precipitation, and even more contingencies. The aerosol appears to change the distribution and intensity of surface rain from deep convective clouds (5); however longer timescale drivers (weeks to months) associated with radiative heating and long-term modification to the surface fluxes by the aerosol could be equally if not more important (6, 7).

Paradigms in Pursuit of Quantification of the Cloud Radiative Effect

The immense complexity of the aerosol itself, the sensitivity of clouds to both meteorological controls and the aerosol, and the co-variability of rapidly changing clouds and aerosol present a particularly challenging problem. As in other studies of complex systems, researchers tend to separate based on academic tradition or discipline into those with a "Newtonian" outlook and those who take a "Darwinian" approach. To paraphrase Harte (8), the Newtonian stresses amongst others, fundamental physical laws, a search for patterns, simple models, and predictive capability based on initial conditions and deterministic laws of physics. In contrast, the Darwinian is more cognizant of the system complexity and contingencies, opposes simple models, and addresses smaller, more manageable, or unique pieces of the problem. Harte has argued eloquently for a synthesis of these two approaches for Earth system science. We will attempt to argue the same as a means of advancing our understanding of, and ability to quantify cloud radiative effect

(CRE)*. Threads of this thinking date even earlier to Karl Popper's work on physical determinism and human behavior, eloquently presented in an essay entitled "Of Clocks and Clouds" (9) in which he describes complex systems in terms of either "clock-like", predictable systems based on fundamental rules, or "cloud-like" systems characterized by "fuzziness" and unpredictability. Our (open) aerosol-cloud system is by definition nebulous and fuzzy, but nevertheless based on fundamental physics. As in Popper's world, it is characterized by neither pure physical determinism nor pure chaos. Describing it fully therefore requires a synergy of these approaches. In Popper's words *"What we need for understanding rational human behaviour….. is something intermediate in character between perfect chance and perfect determinism; something intermediate between perfect clouds and perfect clocks."* We argue that the same is true for complex *physical* systems.

Our motivation is two-fold: 1) to improve our understanding of *cloud-controlling parameters* and *cloud albedo-controlling parameters* with a goal of improving representation of these processes in atmospheric general circulation models (AGCMs); and 2) observational quantification of the aerosol-cloud radiative effect with a focus on process-level understanding. This paper will offer a retrospective of some older approaches to quantification, together with some new ones to illustrate how the community might reorganize how it thinks about the aerosol-cloud problem. The ideas herein draw on many in the published literature so that this work stresses methodology rather than novelty.

* The cloud radiative effect refers to the difference between 'all sky' (cloudy + clear sky) and 'clear sky'

To present our ideas we deal solely with warm (liquid water) clouds, whose dominant influence on radiation is in the shortwave, and for which there is abundant qualitative evidence, but insufficient quantification of an aerosol influence.

Examples

Within sub-disciplines, researchers have traditionally focused on fundamental understanding by addressing parts of the problem. However, the interactions between these components and the implications for climate scale phenomena lend themselves to broader consideration of the environment in which the clouds evolve (dynamics), and the couplings between dynamics, aerosol/cloud microphysics, and radiation. Twomey's (2) landmark paper on aerosol brightening of clouds drove a generation of scientists to try to quantify cloud brightening, whereas today the focus has shifted to the dynamical adjustments of the system that occur in response to such brightening, and whether they amplify (3) or diminish (1, 10) such brightening.

Just a few decades ago it was common to use a cloud model to study a single cloud cell or a subset of cloud processes (Darwinian) whereas today one can simulate a field of clouds based on the same fundamental physics and attempt to project results onto other cloud systems (Newtonian). However, in adding more physics and process interactions, the system rapidly becomes complex enough that the Newtonian approach falls short of being fully explanatory, or able to untangle all causal relationships. The 'tug of war' between fundamental physics projected to the system, and system-wide behavior that has driven detailed analysis of subcomponents of the system can be exemplified in the

following. Suppose one would like to quantify the relationship between planetary albedo (R) and aerosol emissions (E). An equation for this relationship can be broken down via the Chain Rule (11) as:

$$\Delta R = R\frac{d\ln R}{d\ln\tau}\frac{d\ln\tau}{d\ln N_d}\frac{d\ln N_d}{d\ln \mathrm{CCN}}\frac{d\ln \mathrm{CCN}}{d\ln E}\Delta\ln E \quad (1)$$

where τ is cloud optical depth, N_d is drop concentration, and CCN is cloud condensation nucleus concentration.[†] Depending on discipline and expertise the community has coalesced around quantifying individual components of this expansion, both in models, as a means of identifying differences between model representations of said components in a present-day minus pre-industrial sense, and through observations, where the terms are assessed based on present-day measurements.[‡] Addressing any given component of Eq. 1 requires further expansion, e.g.:

$$\frac{d\ln\tau}{d\ln N_d} = \frac{1}{3}\left[1 + 2\frac{d\ln L}{d\ln N_d} + \frac{d\ln k}{d\ln N_d} + 3\frac{d\ln H}{d\ln N_d}\right] \quad (2)$$

where L is liquid water path, k represents drop size distribution breadth, and H is cloud depth. Like the progressive unpeeling of layers of an onion, these terms themselves require further expansion and quantification. Unfortunately the nature of our measurement systems means that there are large uncertainties associated with the terms in Eq. 2, both in magnitude and even in sign. Physical retrievals of the various parameters are often fraught with instrumental or measurement error and assumptions. Individual

[†] This equation assumes a cloudy column, i.e., there is no influence of the aerosol on cloud fraction. While this is unrealistic, the equation is simply used to expound an idea (presented below) rather than for purposes of quantification.

[‡] The relationship between radiative forcing and effect could be addressed with a kernel method (12). The assumption that radiative forcing calculated based on present day aerosol-cloud interactions is equivalent to forcing based on present day minus pre-industrial aerosol might result in a low bias in forcing (13).

terms are poorly constrained and errors compound to yield great uncertainty. For example, in (14) the authors state that although their data generally conform to the expansion in Eq. 2 quite well, they do so because of compensating errors in individual terms. In addition, the sometimes disparate measurement scales, and scales of aggregation associated with different platforms or instruments can further confound quantification (15). Given our current ability to quantify through observations the components in Eqs. 1 and 2, if Eq. 1 or some sub-component like Eq. 2 were to match a proposed theory, how confident could one be in the suitability of that theory?

An alternative approach is to shift attention to observations of system-wide variables that are more closely related to CRE, and for which uncertainties are better known. One example is the relationship between scene albedo A (cloudy plus clear sky portions) and cloud fraction f_c, expressed as (16, 17)

$$A = A_c f_c + A_s (1 - f_c), \quad (3)$$

where A_c is cloud albedo and A_s is surface albedo. A_c is itself a function of τ, and therefore L and N_d. Approximately linear relationships between MODIS-derived f_c and CERES-derived A in multiple marine stratocumulus locations have been found when averaging over 2.5° x 2.5° and one-month periods (18)[§]. Regardless of the exact form, the (A, f_c) relationship has distinct advantages: it can be addressed with fewer measurements than the Chain Rule expansions; measurement error and uncertainty are more directly linked to CRE; measurements can be made from space and from the ground (19, 20); and it captures important underlying physics (21, 22). It is currently used as a means of

[§] Based on Eq. 3, linearity suggests an independence of A_c and f_c.

diagnosing AGCM performance (17, 18) but as we will argue below, could be applied to process models as well.

The (A, f_c) relationship therefore provides a key element of the merged Newtonian-Darwinian approach, i.e., it is an expression of *scaling* (Harte's "Search for Patterns and Laws"). But does it exhibit another very desirable property, namely self-similarity or scale-independence, e.g., does the (A, f_c) relationship vary with spatial or temporal averaging scale? Does it vary across cloud regimes? And if so, can one directly trace the variability to physical processes? Some of these themes will be addressed, albeit briefly, below.

One might argue that in examining relationships such as (A, f_c) rather than (τ, N_d), we are simply shifting the unknown(s) elsewhere. We counter that assessing uncertainties in a higher-level relationship like (A, f_c) is more productive than getting entangled in similar uncertainties in lower-order relationships. Are we abrogating our fundamental intellectual need or mandate to understand and predict all subcomponents of the system? We argue that the broader view, in combination with an appropriate balance of process-level understanding has been particularly productive in other fields. As an illustration, consider the study of *emergence*, another nexus of the Newtonian and Darwinian approaches. Complex pattern formation sometimes emerges from simple deterministic interactions between components of the system. Atmospheric Rayleigh-Bénard convection is one such example that links fundamental process to pattern. Emergence, or pattern formation

provides useful constraints on simulation of deterministic systems and opens rich opportunity for the pursuit of understanding pattern structure and its evolution.

This leads to yet another aspect of Newtonian/Darwinian merging, namely the development of simple, falsifiable models that can be tested in a range of conditions and locales. By illustrating the limits of physical determinism, the system of three coupled differential equations of (23) has been particularly enlightening. This search for simplicity runs counter to the current trend towards ever increasing model complexity – often to the point of attempting to represent complex interactions in models that do not adequately represent the individual components, let alone their interaction. Mixed layer models (24) and simple budget models (25) prove to be very useful, and are able in some cases to reproduce temporal (26) and spatial (27) emergence. By focusing on spatiotemporal patterns, the study of emergence naturally lends itself to simple models. While this topic is of great interest, it will not be developed here.

Here we will attempt to balance Newtonian determinism and Darwinian (real world system) complexity, particularly with an eye to scaling properties. The examples to be presented focus on albedo and radiative effect; precipitation is only discussed to the extent that it affects albedo. Simple models or computationally efficient models will be alluded to, where appropriate. We start with a set of idealized numerical simulations using a cloud resolving model (CRM) and a large eddy simulation (LES), and progress to discussion of a more ambitious project connected tightly to real-world simulation and observation.

Results

Simulations

We use a numerical model, the System for Atmospheric Modeling (SAM (28)). To explore the robustness of the (A, f_c) relationship we apply it to a variety of cases including nocturnal marine stratocumulus (both closed- and open-cell), stratocumulus evolving with the diurnal cycle, and a stratocumulus to cumulus transition case. The simulations are separated into 'nocturnal' and 'diurnal' and described below.

1. Marine stratocumulus: nocturnal simulations

These simulations focus on the sensitivity of cloud albedo A_c, cloud fraction f_c, and liquid water path L to the initial conditions, i.e., they directly address the question of CRE-controlling parameters without considering CRE itself. This is clearly unrealistic but will be used to make some salient points. The model output comprises 220 simulations of marine stratocumulus cloud systems. SAM is initiated with different initial conditions, described in terms of six key parameters: total mixing ratio q_t, liquid water potential temperature θ_l, the depth of the mixed layer H_{mix} over which q_t and θ_l are well-mixed, q_t and θ_l jumps at the inversion, Δq_t, $\Delta\theta_l$, respectively, and aerosol concentration N_a. The ranges of these parameters are: $6.5 < q_t < 10.5$ g kg^{-1}; $284 < \theta_l < 294$ K; $-10 < \Delta q_t < -6$ g kg^{-1}; $6 < \Delta\theta_l < 10$ K; $500 < H_{mix} < 1300$ m; $30 < N_a < 500$ cm^{-3}. Only those initial profiles sampled from the q_t, θ_l, H_{mix} parameter space with L in the range 30 – 200 g m^{-2}, and cloud base in the range 250 – 1100 m were selected for simulation. The parts of the parameter space excluded, which are dependent on a three-dimensional combination of q_t, θ_l, and H_{mix}, are areas/combinations where the simulation would be very unlikely to

produce the cloud-type of interest. Hence, we do have some pre-determined correlation between input parameters q_t, θ_l, and H_{mix}. The domain is 40 km x 40 km x 1.6 km, the grid volume is 200 m x 200 m x 10 m.

We perform two groups of simulations, each with a different method of sampling the initial conditions from the six-dimensional parameter uncertainty space that defines the parameter ranges and constraints. Each group of simulations is allowed to sample from the same ranges of the input parameters q_t, θ_l, H_{mix}, Δq_t, $\Delta\theta_l$, and N_a. The first group of 100 simulations (Set 1) was sampled randomly from a six-dimensional grid covering the meteorological and aerosol parameter space. About 40 of the 100 simulations apply the full range of N_a at fixed meteorology. The second group of 120 simulations (Set 2) was sampled using the maximin Latin hypercube design algorithm (29). It maximizes the minimum distance between selected points to ensure optimal coverage of the multi-dimensional parameter space, which is difficult to obtain manually. Hence, a wider area of the multi-dimensional parameter space is covered in Set 2 than in Set 1. Unlike Set 1, Set 2 has no predetermined correlation between the meteorological drivers (q_t, θ_l, H_{mix}, Δq_t, and $\Delta\theta_l$,) and N_a.

Thus, the manner in which the six input parameters co-vary differs between the two sets. Because meteorology and aerosol typically co-vary in somewhat predictable ways, neither of the methods is a realistic sampling of what the atmosphere presents, (except for the realistic range over which the parameters are varied), but as will be demonstrated below they serve our purpose well.

2. Marine stratocumulus and stratocumulus-to-trade cumulus transition: diurnal simulations

Here the focus is on CRE, A, and f_c. A random sample of 15 of the 220 nocturnal simulations are repeated for a period of 10 h with a 04:00 LT start time and a diurnal cycle of radiation. Radiative calculations are applied in each model column. In addition, a composite sounding based on NE Pacific Lagrangian trajectories (30) is used to simulate a transition case in the presence of (absorbing) smoke aerosol residing some distance above, and later entrained into cloud. Forcings, including a gradual increase in sea surface temperature, are applied (30). For this transition case, the shortwave (SW) heating associated with the aerosol is also coupled to dynamics (31). A solid stratocumulus to broken cumulus transition is simulated over the course of 3 days; initial smoke conditions are either low N_a (aerosol optical depth $\tau_a = 0.06$) or high N_a ($\tau_a = 0.50$). The asymmetry parameter is 0.67 and the single scattering albedo ω_o is 0.80 (at 0.5 μm), representing smoke mixed with hygroscopic material (31). Such a low value of ω_o is associated with fresh smoke and is perhaps unrealistic. It does, however serve to test the sensitivity of the (A, f_c,CRE) phase space to aerosol absorption. The model is run on a 12 km x 12 km x 4 km domain with a grid volume of 50 m x 50 m x 10 m.

Simulation Results

1. Marine stratocumulus: nocturnal simulations

A scatterplot of the domain mean cloud albedo $\bar{A}_c$ as a function of the six input parameters is shown in Fig. 1 for Set 1. Each point represents an hourly average over

hour six of the simulation, and is colored by L. A_c is calculated from τ using a two-stream approximation (32). Ignoring the coloring by L one immediately sees that there is no simple dependence of $\bar{A}_c$ on individual parameters. Sorting by L does bring out some distinct patterns, which is particularly clear for $\bar{A}_c$ vs. N_a. This is an expression of the albedo susceptibility relationship, calculated at constant L: $S_a = \partial A_c/\partial N_d = A_c(1-A_c)/3N_d$ (33); slopes for given L in Fig. 1f are maximum at small N_d and $\bar{A}_c \sim 0.5$. $\bar{A}_c$ is also shown to depend strongly on L and f_c (Figs. 1g, h). A partial multivariate linear correlation of $\bar{A}_c$ vs. the six input parameters[**] produces correlation coefficients of 0.44 (q_t), -0.56 (θ_l), 0.58 (H_{mix}), -0.32 (Δq_t), 0.35($\Delta\theta_l$), and 0.67 (ln N_a). Thus all input parameters contribute significantly to $\bar{A}_c$.

We now calculate A as in Eq. 3 with $A_s = 0.08$ (for ocean), and A_c and f_c based on $\tau > 0.2$[††]. Points are domain average values, colored by input N_a. One sees (Fig. 2) a weak, but distinct separation of colors indicating that for given f_c higher N_a tends to result in higher A. Figure 2 also includes calculations based on 3-D radiative transfer modeling of four individual snapshots of cloud fields from an independent simulation (four red '+' signs) (34). The location of these points is close to those from the two-stream approximation suggesting that details of the A calculation appear to have a small influence. There is, however, a distinct sensitivity to the definition of f_c : the red '+' signs calculate f_c based on $\tau > 0.2$ while the black '+' sign calculates f_c for $\tau > 0.1$.

[**] i.e., a correlation between $\bar{A}_c$ and any one of the six parameters with the effects of the others removed.
[††] the $\tau > 0.2$ criterion was chosen for consistency with 3-D calculations in Fig. 2.

A line approximating monthly mean 2.5° x 2.5° results for a MODIS Terra measurement from Californian stratocumulus (18) is superimposed for reference. Except for the bounding by A_s at $f_c = 0$ and by A_c at $f_c = 1$, there is no *a priori* reason why the relationship based on the small spatiotemporal averaging in this work should behave similarly to that from the large spatiotemporal averaging as in (18); differences between the CRM output and the remote sensing data are likely related, amongst others, to the averaging scale, co-variability in meteorology and aerosol (cf. Figs. 2 and 4), and definition of f_c (*SI Text*, Fig. S1). The relative robustness of the (A, f_c) relationship reinforces our point that well-defined higher-level relationships are preferred over uncertain, poorly constrained lower level ones. Effort to understand the connection between the form of the (A, f_c) relationship and its controlling factors would therefore seem profitable.

Figures for Set 2 show similar behavior for the scatter plots in terms of the individual inputs (Fig. 3). The robust relationships are again reflected in $\bar{A}_c$ vs. L and f_c. Applying Eq. 3, the A vs. f_c relationship is highlighted again (Fig. 4), this time with f_c and A_c based on $\tau > 1$. Here there is almost no discernible influence of N_a on A at constant f_c, regardless of how f_c and A_c are defined (See *SI Text* and Fig. S2). Moreover, both high and low N_a are intermingled over a range of A and f_c. While these two sets of simulations sample from the same range of initial conditions, they differ (i) in the manner in which the six input parameters are sampled, and (ii) in the parameter space covered by the sampling. Unlike Set 1 there is almost no repetition of meteorological conditions defined by the input combinations in the Set 2 simulations. This brings out an important point: *the*

influence of the aerosol on albedo at constant f_c depends on the co-variability of meteorology and aerosol. This is a result supported by observational studies that have underscored the difficulty in separating meteorological and aerosol influences on A because variability in A is overwhelmed by variability in f_c and L (21). The (A, f_c) phase space is a useful way of demonstrating this, and there is a clear need for realism in the sampling of the co-varying initial conditions if we are to discern aerosol influences. The frequently used modeling strategy where N_a is varied for given meteorology should not be applied, and demonstration of an aerosol response in this framework is not an indication of realistic response, unless of course nature presents such conditions.

It is worth noting that low N_a is often associated with precipitation-induced cloud breakup. Thus to the extent that N_a controls precipitation in these systems it has the potential to strongly affect A and f_c, by moving points towards the lower left of the (A, f_c) trace. Here too, differences between Set 1 and Set 2 are distinct; In Fig. 2 points with low N_a and low f_c are more common than in Fig. 4.

2. Marine stratocumulus and stratocumulus-to-trade cumulus transition: diurnal simulations

These simulations include part of the diurnal cycle so that the broadband SW CRE can be calculated over the course of 10-h for the stratocumulus simulations, and 3 days for the transition cases. To simplify analysis we calculate relative cloud radiative effect (rCRE):

$$\mathrm{rCRE} = 1 \; - \; \frac{F_{sw,all}}{F_{sw,clr}} \qquad (4)$$

where F_{sw} denotes net SW surface fluxes, *all* denotes 'all-sky' and 'clr' denotes clear sky. Measurement of rCRE was developed for surface-based measurements (19), and by normalizing, focuses on clouds, without the confounding effects of solar angle or surface albedo.

Here rCRE calculations are performed based on Eq. 4 during daylight hours when SW fluxes are calculated. rCRE is shown as a function of f_c (based on $\tau > 1$; Fig. 5a) and scene albedo A (Fig. 5b) for the composite of 15 stratocumulus (1-h snapshots) and 2 transition simulations (low τ_a and high τ_a), also at hourly intervals. Such analyses show the relative importance of intrinsic factors (A) or extrinsic factors (f_c) in controlling rCRE (20, 22). It is immediately clear that the simulations tend to follow a fairly robust relationship, with rCRE, as expected, increasing progressively with increasing f_c and A. The low τ_a transition case output (filled circles) follows the stratocumulus (filled squares) cases quite well in spite of the large differences in initial soundings and system evolution. The points from the high τ_a smoky transition case tend to lie below the main branch of stratocumulus points (Fig. 5b, diamonds); at low f_c they illustrate the brightening of the dark ocean surface by the aerosol. The few scattered (diamond) points at the very highest rCRE and A are associated with smoke-influenced clouds with very high N_a and N_d.

Model output from Figs. 5ab, this time in (A, f_c) phase space with points colored by rCRE (Fig. 5c), again show the characteristic path in (A, f_c) space. Note that points with similar A and f_c may have significantly different rCRE because they are associated with different cloud and aerosol conditions. While we make no claims on the universality of relationships such as those in Fig. 5, the robustness suggests that the (A, f_c) phase space is

a useful one for exploring controls on rCRE (or CRE) and linking physical processes and assumptions made in the analysis to rCRE patterns.

A Path Forward

Results emphasize the influence of the co-variability (in six-dimensional space) of initial conditions/cloud controlling parameters on key cloud field attributes. Two sampling strategies from the same range of initial conditions produce different indications of the role of the aerosol. This leads to the question of how the system might respond to a *naturally occurring* co-variability of the inputs. We propose to address this question by repeating large numbers of LES, CRM, and coarser mesh model simulations in specified cloud regimes using initial conditions from *routine observations* (or observationally constrained model output), as in (35) but also including aerosol information. Initial conditions could be based on radiosondes or from reanalysis, daily Numerical Weather Prediction (NWP) derived soundings, or Variational Analysis (36). Model output that successfully[‡‡] reproduces a desired set of observed quantities, which should include surface shortwave radiation, L, f_c, A_c, can then be tied to the observed initial meteorological conditions, N_a, and surface latent and sensible heat fluxes. Given that observed profiles will differ from the idealized mixed layer profiles used here, classification of observed profiles in terms of key characteristics will likely be necessary. A large number of simulations will then allow one to explore the relationship between input profiles and CRE, A_c, f_c, L, and N_a.

[‡‡] "Successful" is defined ad hoc. For a radiation-centric study a successful simulation would need to compare sufficiently well to measurements of, *inter alia*, surface shortwave radiation, τ, f_c, and L. As in (37) the unsuccessful simulations provide opportunity for model improvement (both LES and SCM).

Analyses of successful model output in (CRE, A, f_c) space will allow a methodical, process-based link to observed environmental and aerosol conditions with a hierarchy of models, but importantly will include small-scale process models. Because individual microphysical and macrophysical responses to the aerosol can also be measured from the surface and from satellites, there is benefit in examining, in parallel, individual response terms $d\ln X/d\ln N_a$ (e.g., Eq. 2), and comparing model output and observations at multiple levels. Agreement at multiple levels will provide further confidence in the fidelity of simulations. Nevertheless we urge appropriate balance in these higher- and lower-order efforts given the measurement uncertainties and imperfect model physics.

Routine LES has been demonstrated for improving single column model (SCM) physics, thus providing a direct path to improving AGCM physics (37). The U.S. Department of Energy's Atmospheric Radiation Measurement Program (DOE/ARM) will soon embark on a pilot study to perform routine LES at the Southern Great Plains (SGP) site in Oklahoma (38), and a European project (High Definition Clouds and Precipitation for Climate Prediction; http://www.hdcp2.eu/) has similar goals of routine, integrated modeling and observation. In addition to SCM simulations, AGCMs could directly benefit if they are initialized with the same inputs and run in hindcast mode over short periods of time (39). A schematic of the approach is shown in Fig. 6. This effort should be performed in key cloud regimes such as stratocumulus, cumulus, and the stratocumulus-to-cumulus transition. For deep convective clouds, CRE calculations require other considerations.

Emulators

LES and even CRM is computationally expensive, so pursuit of a physically or perhaps statistically based simpler model with a limited number of free parameters is of great interest. These simpler representations would be designed to emulate LES or CRM results, and explain the sensitivities of key outputs such as A_c, f_c, CRE, and L to the initial conditions. Simplified budget models and statistically based emulators (40, 41) have been proposed. The two aforementioned studies assessed the uncertainty of key model outputs with respect to uncertainty in model parameters representing physical processes. Rather than assess sensitivity to model parameters, here the emulator will be used to relate variations in A, f_c, and CRE to meteorological and aerosol drivers. The construction of an emulator requires optimal coverage of the parameter space in the sample of model runs using e.g., the maximin Latin hypercube approach (hence the use of this sampling method for Set 2; Figs. 3 and 4). These 120 simulations are currently being used to construct emulators, and are showing promise. The greatest challenge is the sometimes steep local slope in six-dimensional input parameter space, meaning that small changes in input parameters have a large influence on the outcome. A successful emulator would ultimately use as input the observed co-varying initial conditions and would, at minimal computational expense, allow a much denser sampling of parameter space than the LES or CRM. Emulators would have to be reconstructed for different cloud regimes. To the extent that this experiment is successful, emulation could serve as a very useful method for relating initial conditions to CRE, A, and f_c outcomes in different cloud regimes. Moreover, the output parameters are all measureable, which means that the emulator

could be tested against observations in parts of the input space not used to train the emulators.

Summary

The proposed analysis framework combines our penchant for Newtonian determinism in the form of cloud system modeling that resolves key physics; addresses scale-dependence; seeks emergent phenomena; and pursues simple models, with the Darwinian recognition that our system is fundamentally unpredictable, and can not be addressed purely deterministically. The approach shifts the balance of effort from low-order observational constraints that are highly scale-dependent and suffer from instrumental or retrieval error, towards constraints on higher-order parameters that are fundamental to the cloud radiative effect. The latter, expressed here as an (A, f_c) relationship and CRE = $f(A, f_c)$, are not without uncertainty but by addressing them at this higher level we avoid excessive compounding, or unwanted offsetting of errors.

Numerical simulation of warm cloud systems has been used to demonstrate that the manifestation of aerosol effects on A and f_c depends on the co-variability of meteorology and aerosol. We note, however, that even when aerosol effects on albedo at constant f_c are overwhelmed by other factors (e.g., Fig. 4) that aerosol effects on precipitation may still provide a strong control on A and f_c (34), and this avenue for the radiative effect of the aerosol still appears to be pivotal. (A, f_c) trajectories have been shown to be relatively robust but show some sensitivity to co-variability of initial conditions, meteorological regime, and averaging scale. Their scaling properties therefore deserve attention. They

are also sensitive to the definition of f_c (Fig. 2 and *SI*), an issue raised in various other works (42). Analyses should therefore always be associated with clear criteria for definition of f_c.

We amplify the call for routine LES driven by observed simultaneously varying meteorological *and* aerosol conditions to clarify the relationship between co-variability in aerosol and meteorology, and the (A, f_c, CRE) phase space in a process model framework. Current efforts at elucidating this relationship rely on reanalysis (21, 22), and while the latter approach is valuable at the regional circulation scale, reanalysis is not reliable enough at the cloud scale. Model-observation comparison at the level of individual microphysical and macrophysical responses to the aerosol (Eq. 2) will provide further confidence in the fidelity of simulations.

As noted elsewhere (37), routine LES provides a mechanism to rigorously evaluate models against a desired set of output parameters. Successful simulations (based on prescribed tolerances) form an observationally constrained model output, which could be used for multiple other analyses similar to the various Model Intercomparison (MIP) projects.

One of the tenets of the merging of Newtonian and Darwinian world-views somewhat neglected here is the development of simple models. This merging is itself recognition of the imperfection of Popper's "clocks". Lorenz's model (23) epitomizes the merged approach because it not only captures the spirit of the merging, but also highlights the

imperfection of the "clock" through its identification of sensitivity to initial conditions. Statistical emulator models are far from simple, and do not provide process level understanding like a simple model does. However, when designed with, and driven by the appropriate regime-based conditions, they may be an expedient and pragmatic tool for filling in gaps and extending our ability to represent the aerosol-cloud system in different regimes. Simple, transparent models (8, 43) should be considered in parallel.

Acknowledgements

The authors thank the Sackler Colloquium for the opportunity to present these ideas. Funding was provided by NOAA's Climate Goal and the U.S. Department of Energy, Office of Science, Biological and Environmental Research under the Atmospheric System Research (ASR) Program (Grant #s DE-SC0006972 and DE-SC0008112).

References

1. Stevens B, Feingold G (2009) Untangling aerosol effects on clouds and precipitation in a buffered system. *Nature* 461: 607-613.
2. Twomey S (1977) The influence of pollution on the shortwave albedo of clouds. *J Atmos Sci* 34(7): 1149-1152.
3. Albrecht B (1989) Aerosols, cloud microphysics, and fractional cloudiness. *Science* 245: 1227–1230.
4. Lee S-S, Feingold G, Chuang PY (2012) Effect of aerosol on cloud-environment interactions in trade cumulus. *J Atmos Sci* 69: 3607-3632.
5. Parodi A, Foufoula-Georgiou E, Emanuel K (2011) Signature of microphysics on spatial rainfall statistics. *J Geophys Res* 116, D14119.
6. Bollasina MA, Ming Y, Ramaswamy V (2011) Anthropogenic Aerosols and

the Weakening of the South Asian Summer Monsoon. *Science* 334: 502-505.

7. Lau K-M, Kim M-K, Kim K-M (2006) Asian summer monsoon anomalies induced by aerosol direct forcing: The role of the Tibetan Plateau. *Climate Dyn* 26: 855–864.
8. Harte J (October 2002) Towards a synthesis of the Newtonian and Darwinian worldviews. *Phys Today* 29–34.
9. Popper KR (1965) "Of Clocks and Clouds: An approach to the problem of rationality and the freedom of man," the Arthur Holly Compton Memorial Lecture presented at Washington University, April 21, 1965 (St. Louis: Washington University, 1966). [Available in Popper, K.: Objective Knowledge: An Evolutionary Approach, Oxford University Press, USA, revised edn., 1972.]
10. Wood R. (2007) Cancellation of aerosol indirect effects in marine stratocumulus through cloud thinning. *J Atmos Sci* 64: 2657-2669.
11. Ghan S, Wang M (2015) Presented at DOE/ASR Science Team Meeting March 17 2015. Available at http://asr.science.energy.gov/meetings/stm/2015/presentations/Tuesday-PlenaryAM-8-CAPI.pdf [*also a submission to this issue*].
12. Taylor KE et al. (2007) Estimating shortwave radiative forcing and response in climate models. *J Clim* 20: 2530-2543.
13. Penner JE, Xu L, Wang M (2011) Satellite methods underestimate indirect climate forcing by aerosols. *P Natl Acad Sci* 108: 13404 - 13408.

14. Ackerman AS et al. (2000) Effects of aerosols on cloud albedo: Evaluation of Twomey's parameterization of cloud susceptibility using measurements of ship tracks. *J Atmos Sci* 57: 2684-2695.
15. McComiskey A, Feingold G (2012) The scale problem in quantifying aerosol indirect effects. *Atmos Chem Phys* 12: 1031 - 1049.
16. Charlock TP, Ramanathan V (1985) The albedo field and cloud radiative forcing produced by a general-circulation model with internally generated cloud optics. *J Atmos Sci* 42(13): 1408–1429.
17. Webb M, Senior C, Bony S, Morcrette JJ (2001) Combining ERBE and ISCCP data to assess cloud in the Hadley Centre, ECMWF and LMD atmospheric climate models. *Climate Dynamics* 17: 905-922.
18. Bender, F A-M, Charlson RJ, Ekman AML, Leahy V (2011) Quantification of Monthly Mean Regional-Scale Albedo of Marine Stratiform Clouds in Satellite Observations and GCMs. *J Appl Meteor Climatol* 50:2139–2148.
19. Betts AK (2007) Coupling of water vapor convergence, clouds, precipitation, and land-surface processes. *J Geophys Res* 112, D10108, doi:10.1029/2006JD008191.
20. Xie Y, Liu Y (2013) A new approach for simultaneously retrieving cloud albedo and cloud fraction from surface-based shortwave radiation measurements. *Environ Res Lett* 8: 044023 doi:10.1088/1748-9326/8/4/044023
21. George RC, Wood R (2010) Subseasonal variability of low cloud radiative properties over the southeast Pacific Ocean. *Atmos Chem Phys* 10: 4047–

4063.

22. Chen Y-C, Christensen MW, Stephens GL, Seinfeld JH (2014) Satellite-based estimate of global aerosol-cloud radiative forcing by marine warm clouds. *Nature Geosci* 7: 643-646.
23. Lorenz EN (1963) Deterministic nonperiodic flow. *J Atmos Sci* 20: 130–141.
24. Lilly DK (1968) Models of cloud-topped mixed layers under a strong inversion. *Quart J Roy Meteor Soc*, 94: 292–309.
25. Wood R, Leon D, Lebsock M, Snider J, Clarke AD (2012) Precipitation driving of droplet concentration variability in marine low clouds. *J Geophys Res* 117, D19210, doi:10.1029/2012JD018305.
26. Koren I, Feingold G (2011) The aerosol-cloud-precipitation system as a predator-prey problem. *P Natl Acad Sci* 108: 12227– 12232.
27. Feingold G, Koren I (2013) A model of coupled oscillators applied to the aerosol–cloud–precipitation system. *Nonlin Processes Geophys* 20: 1011–1021.
28. Khairoutdinov MF, Randall DA (2003) Cloud resolving modeling of the ARM summer 1997 IOP: Model formulation, results, uncertainties, and sensitivities. *J Atmos Sci* 60: 607-625.
29. Morris MD, Mitchell TJ (1995) Exploratory designs for computer experiments. *J Stat Plann Inference* 43: 381–402.
30. Sandu I, Stevens B (2011) On the factors modulating the stratocumulus to cumulus transitions. *J Atmos Sci* 68: 1865-188.
31. Feingold G, Jiang H, Harrington JY (2005) On smoke suppression of clouds

in Amazonia. *Geophys Res Lett* 32: 10.1029/2004GL021369.

32. Bohren CF (1987) Multiple scattering of light and some of its observable consequences. *American Journal of Physics* 55: 524 – 533.
33. Platnick S, Twomey S (1994) Determining the susceptibility of cloud albedo to changes in droplet concentration with the Advanced Very High Resolution Radiometer. *J Appl Meteor* 33: 334–347.
34. Feingold G, Koren I, Yamaguchi T, Kazil J (2015) On the reversibility of transitions between closed and open cellular convection. *Atmos Chem Phys* 15: 7351 - 7367.
35. Seifert A, Köhler C, Beheng KD (2012) Aerosol-cloud-precipitation effects over Germany as simulated by a convective-scale numerical weather prediction model. *Atmos Chem Phys* 12: 709-925.
36. Zhang MH, Lin JL, Cederwall RT, Yio JJ, Xie SC (2001) Objective analysis of the ARM IOP data: method and sensitivity. *Monthly Weather Review* 129: 295–311.
37. Neggers, RAJ., Siebesma AP, Heus T (2012) Continuous single-column model evaluation at a permanent meteorological supersite. *Bull Amer Meteor Soc* 93: 1389–1400.
38. U.S. Department of Energy. 2014. Atmospheric Radiation Measurement Climate Research Facility – Atmospheric System Research High-Resolution Modeling Workshop, DOE/SC-0169. http://science.energy.gov/~/media/ber/pdf/workshop%20reports/doe-sc-0169-low-resolution.pdf

39. Phillips, TJ *et al.* (2004) Evaluating parameterizations in GCMs: Climate simulation meets weather prediction. *Bull Amer Meteor Soc* 85: 1903 – 1915.

40. Carslaw KS *et al.* (2013) Large contribution of natural aerosols to uncertainty in indirect forcing. *Nature* 503: 67–71.

41. Johnson JS, et al. (2015) Evaluating uncertainty in convective cloud microphysics using statistical emulation. *J Adv Model Earth Syst* 7: 162–187.

42. Charlson RJ, Ackerman AS, Bender F A-M, Anderson TL and Liu Z (2007) On the climate forcing consequences of the albedo continuum between cloudy and clear air. *Tellus B* 59: 715–727.

43. Stevens B (2015) Rethinking the lower bound on aerosol radiative forcing. *J Clim* 28*:* 4794-4819.

Figure Captions

Figure 1: Scatterplot of domain mean cloud albedo $\bar{A}_c$ (sum of A_c normalized by number of columns in domain) as a function of input conditions (a)-(f), and as a function of L (g) and f_c (h). Points are hourly averages over the last hour of a 6-h simulation. A_c is calculated based on cloud optical depth τ (32). Points are colored by L. In (f) the slopes of the dashed lines indicate albedo susceptibility for given L. Slopes are steeper at small N_d and flatten with increasing N_d.

Figure 2: Mean scene albedo A (cloudy plus clear sky) calculated based on Eq. 3 (with A_s = 0.08) as a function of f_c (defined based on $\tau > 0.2$). Points are colored by N_a. The aerosol influences both the cloud and surface albedo. A weak but distinct influence of N_a on A can be seen. Points associated with higher N_a tend to be at higher A and higher f_c. The dotted line is an approximation to the relationship in (18) for 2.5° x 2.5° monthly average data from Californian stratocumulus (MODIS and CERES on Terra). The red '+' signs (not colored by N_a) are from 3-D radiative transfer calculations for four cloud fields associated with a closed cell stratocumulus transitioning to the open-cell state (34), also with f_c defined based on $\tau > 0.2$. The black '+' sign is a recalculation of the red '+' to its left where a weaker condition ($\tau > 0.1$) is applied to the calculation of f_c.

Figure 3: As in Fig. 1 but for Set 2.

Figure 4: As in Fig. 3 but for Set 2. Here f_c and A_c are calculated based on $\tau > 1$.

Figure 5: rCRE calculations in (A, f_c) space for 15 stratocumulus and 2 stratocumulus-to-trade-cumulus transition simulations: (a) rCRE vs. f_c; (b) rCRE vs. A, and (c) A vs. f_c. Symbols: squares represent stratocumulus; circles are for the low smoke τ_a transition case, and diamonds are for the high smoke τ_a transition case. Points represent 1-h snapshots. Here f_c and A_c are calculated based on $\tau > 1$.

Figure 6: Schematic showing systematic comparison between surface and/or satellite remote sensing of key measurements with those produced by high resolution LES and or SCM output. Here the focus is on high level parameters such as A, f_c, and CRE but more detailed comparisons at the level of L, τ, r_e, N_a, and surface fluxes provide further physical consistency checks. The LES and SCM are driven on a routine basis by realistic initial conditions that capture the natural co-variability of aerosol and meteorology. Systematic improvements in SCMs provide a pathway to improved AGCM physics so that climate relevant present day (PD) – preindustrial (PI) calculations can be performed. AGCMs run in hindcast mode with the same input conditions can also be used (CAPT: Cloud-Associated Parameterizations Testbed (39)). VA = Variational Analysis; NWP=Numerical Weather Prediction; RGCM=Regional General Circulation Model.

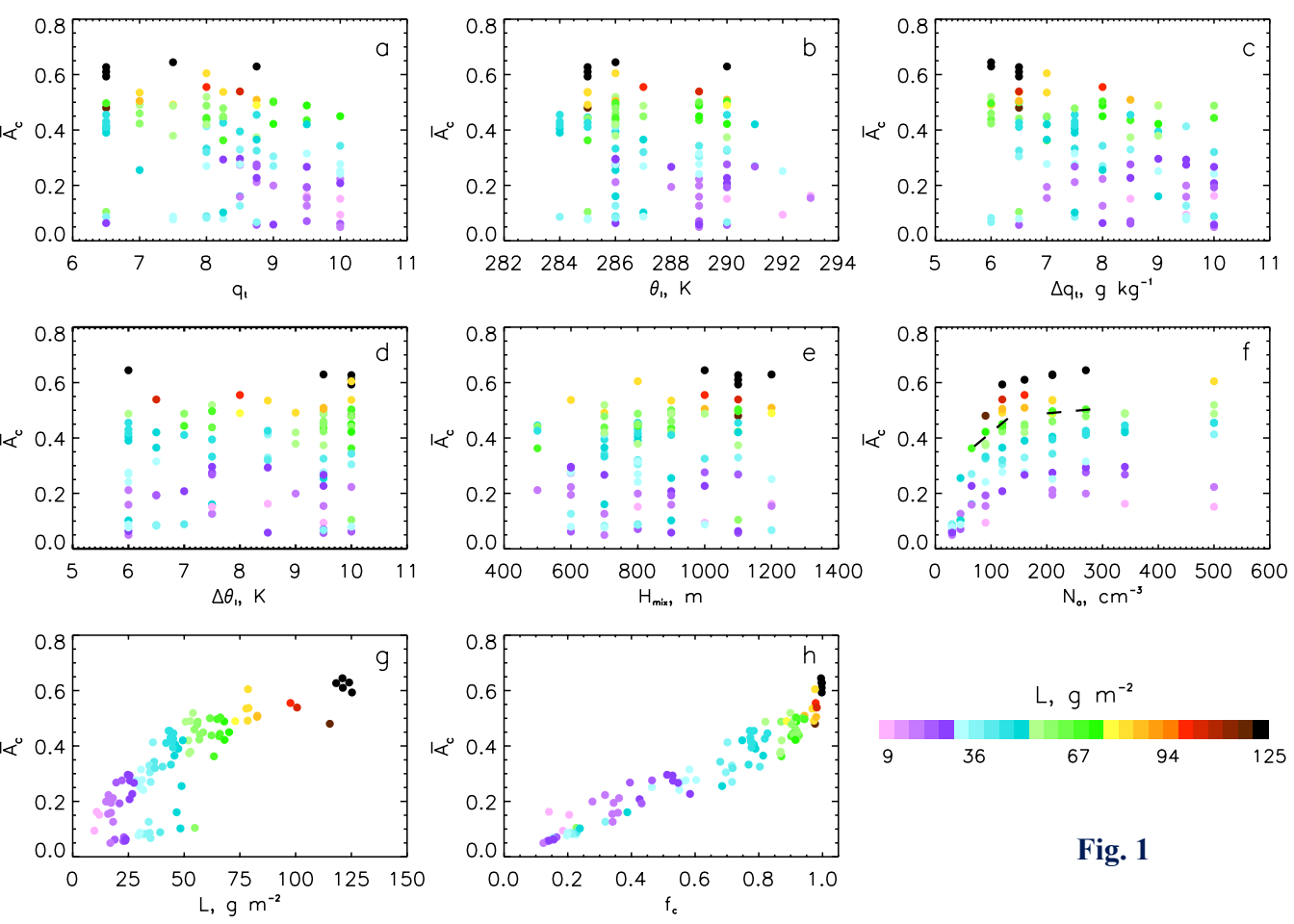
a
b
c
d
e
f
g
h
$\bar{A}_c$
q_t
θ_l, K
Δq_t, g kg^{-1}
$\Delta\theta_l$, K
H_{mix}, m
N_a, cm^{-3}
L, g m^{-2}
f_c
L, g m^{-2}
9
36
67
94
125

Fig. 1

Fig. 2

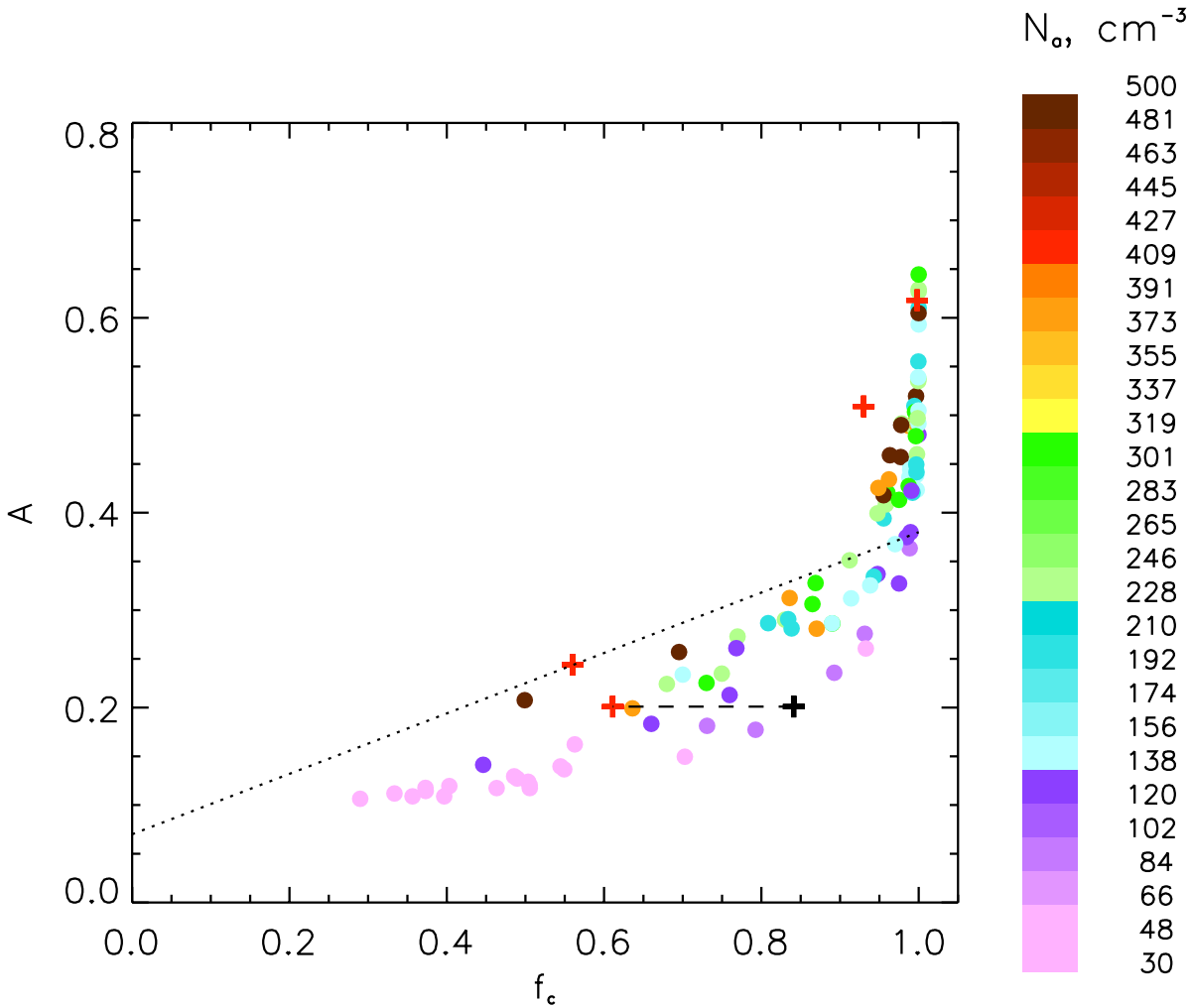
N_o, cm^{-3}
500
481
463
445
427
409
391
373
355
337
319
301
283
265
246
228
210
192
174
156
138
120
102
84
66
48
30
A
0.0
0.2
0.4
0.6
0.8
1.0
f_c

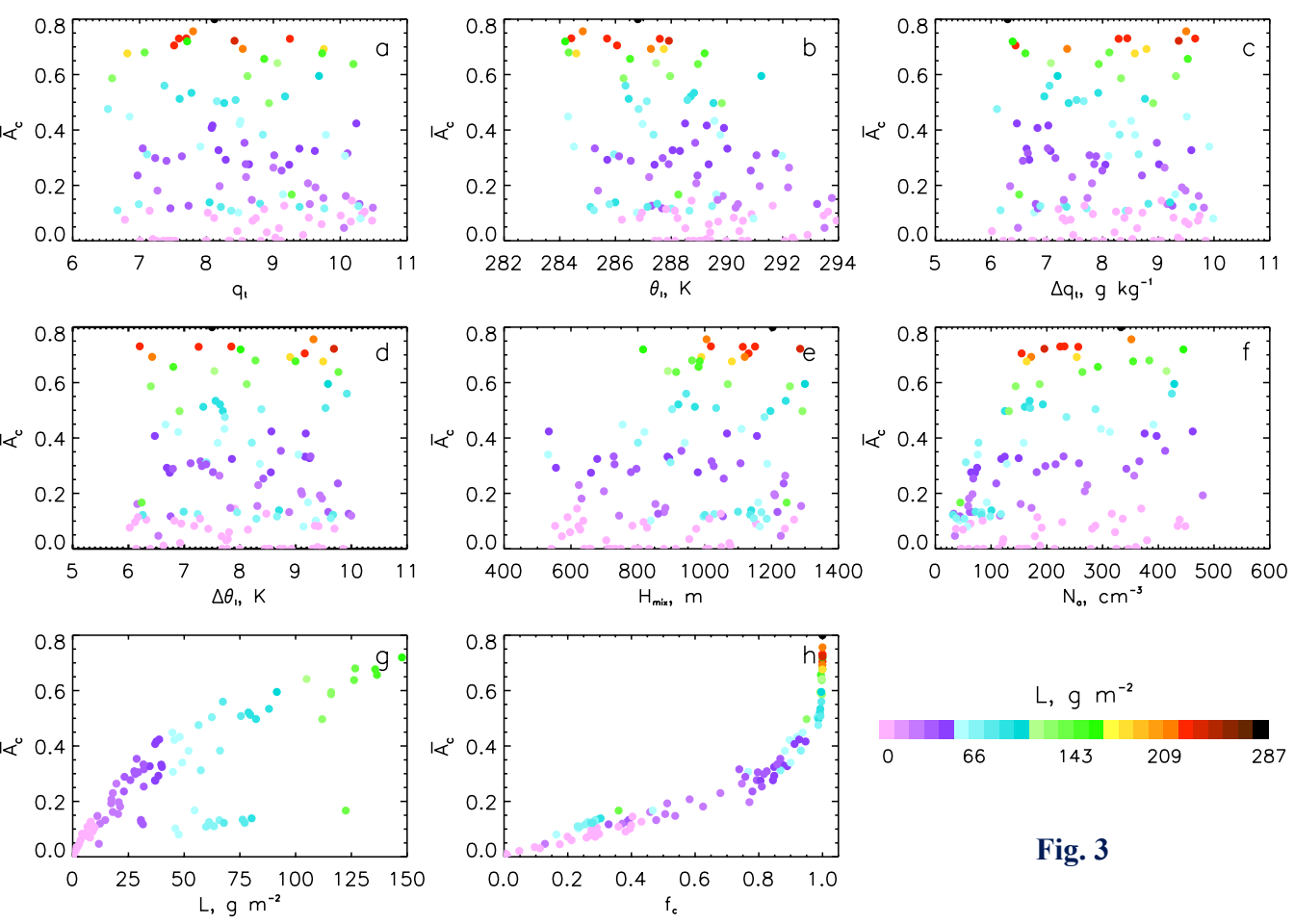
a
b
c
d
e
f
g
h
$\bar{A}_c$
q_t
θ_{ll}, K
Δq_t, g kg^{-1}
$\Delta\theta_{ll}$, K
H_{mix}, m
N_a, cm^{-3}
L, g m^{-2}
f_c
L, g m^{-2}
0
66
143
209
287

Fig. 3

Fig. 4

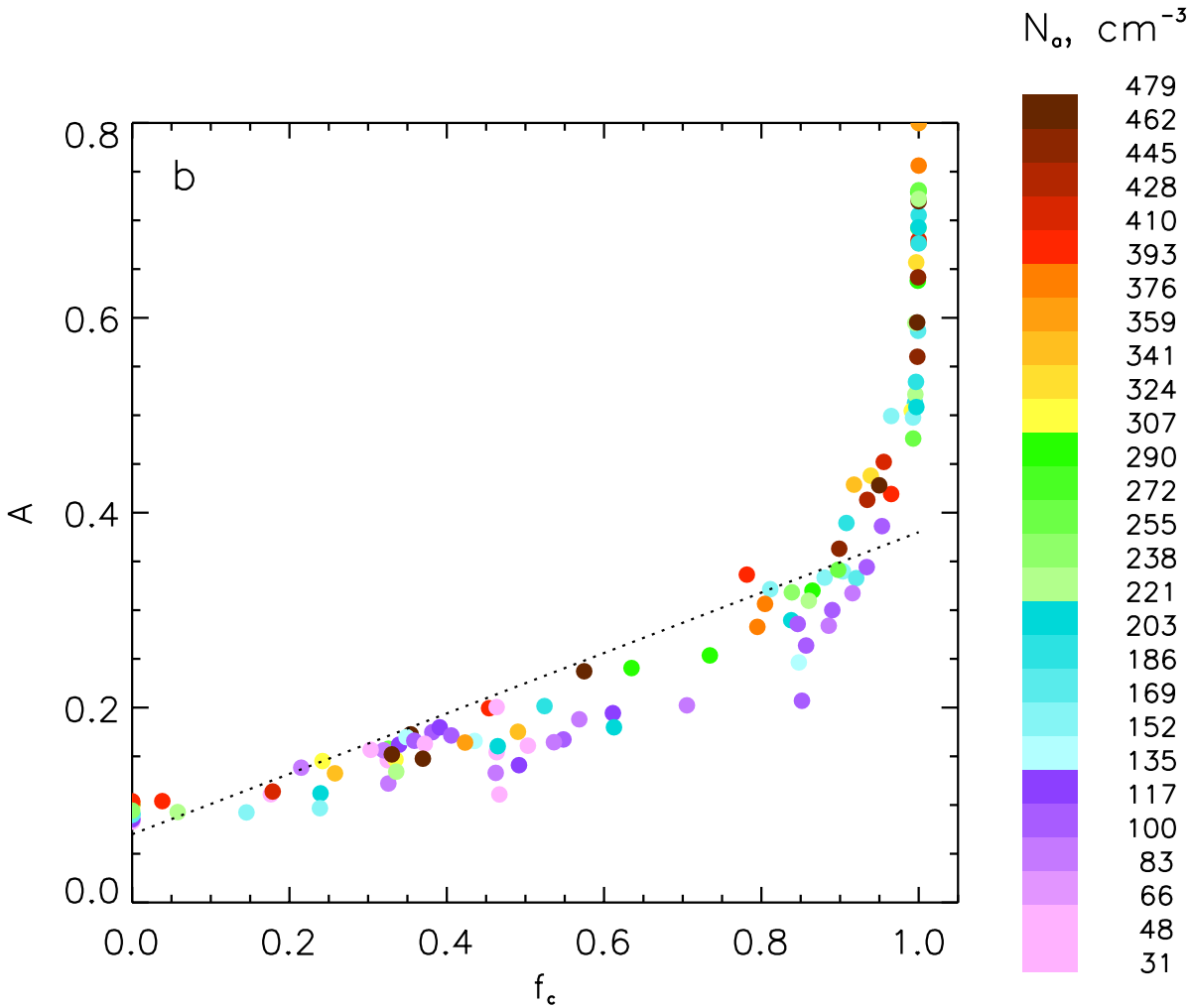
b
A
f_c
0.0
0.2
0.4
0.6
0.8
1.0
N_o, cm^{-3}
479
462
445
428
410
393
376
359
341
324
307
290
272
255
238
221
203
186
169
152
135
117
100
83
66
48
31

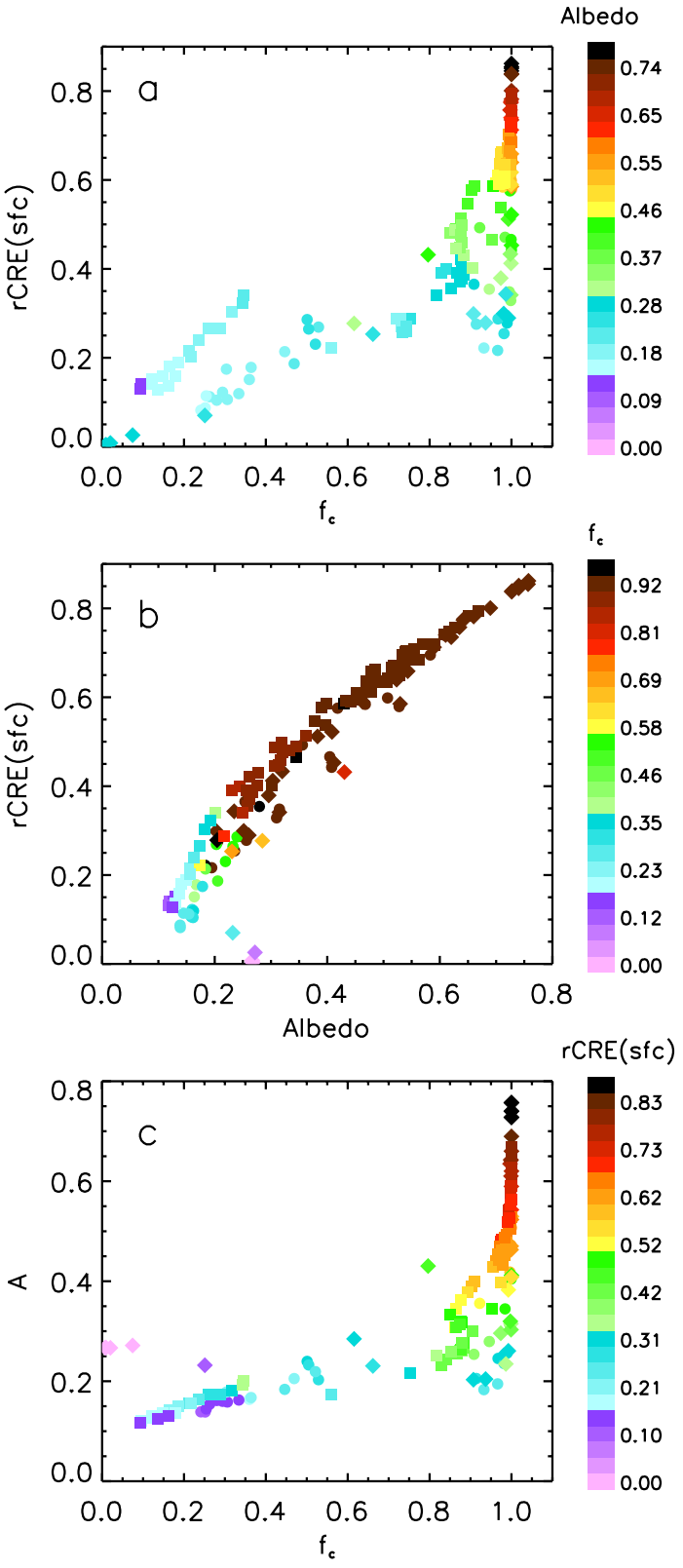
a
rCRE(sfc)
f_c
Albedo
0.74
0.65
0.55
0.46
0.37
0.28
0.18
0.09
0.00
b
rCRE(sfc)
Albedo
f_c
0.92
0.81
0.69
0.58
0.46
0.35
0.23
0.12
0.00
c
A
f_c
rCRE(sfc)
0.83
0.73
0.62
0.52
0.42
0.31
0.21
0.10
0.00

Fig. 5

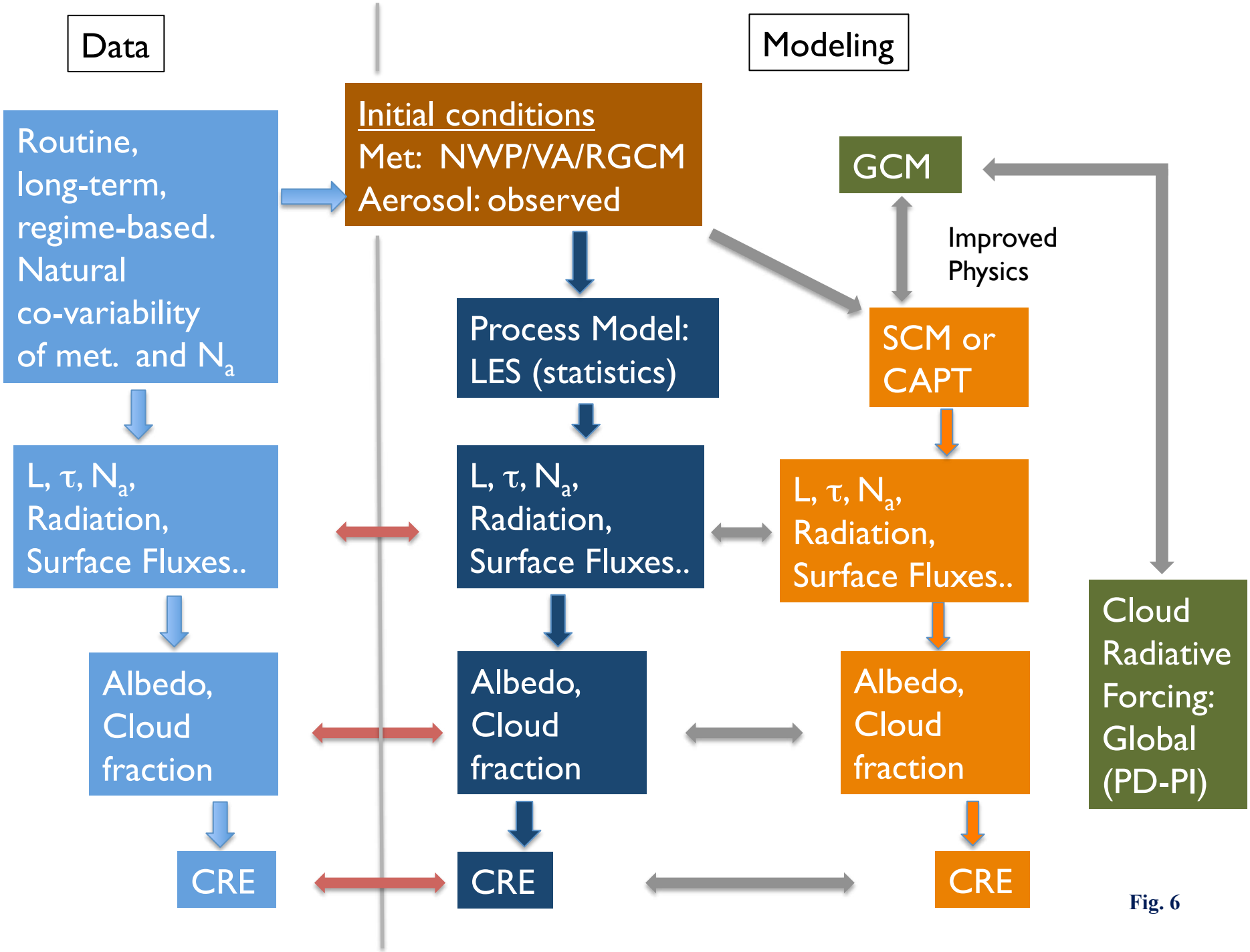
Data
Modeling
Routine, long-term, regime-based. Natural co-variability of met. and N_a
Initial conditions
Met: NWP/VA/RGCM
Aerosol: observed
GCM
Improved Physics
Process Model: LES (statistics)
SCM or CAPT
L, τ, N_a, Radiation, Surface Fluxes..
L, τ, N_a, Radiation, Surface Fluxes..
L, τ, N_a, Radiation, Surface Fluxes..
Albedo, Cloud fraction
Albedo, Cloud fraction
Albedo, Cloud fraction
CRE
CRE
CRE
Cloud Radiative Forcing: Global (PD-PI)

Fig. 6

Supporting Information

Feingold et al.

SI Text

Sensitivity of calculations to definition of cloud fraction f_c

Analysis of Set 1 in Fig. 2 uses a threshold cloud optical depth $\tau > 0.2$ for definition of f_c for consistency with the computationally expensive 3-D radiative transfer calculations (red '+' symbols). Here we reproduce analysis in Fig. 2 using τ thresholds of 1, 2, and 5 to define f_c. As seen in Fig. S1, an increase in the τ threshold shifts more points to low f_c and raises the values of A for $f_c < 1$ as more and more low f_c, weak reflective cloud elements are excluded. As a result the linearity of the (A, f_c) points increases as the τ threshold increases. The weak aerosol influence on A seen in Fig. 2 persists. To compare results for Set 1 and Set 2 using the same definition of f_c, Fig. S1a should be compared to Fig. 4.

The same exercise is repeated for Set 2; for clarity, we reproduce Fig. 4 (f_c based on $\tau > 1$) alongside similar figures that use $\tau > 2$ and $\tau > 5$ to define f_c. Similar trends to those seen in Fig. S1 can be seen. As in Fig. 4, N_a has almost no influence on A.

Figure Captions

Figure S1. Mean scene albedo A (cloudy plus clear sky) for Set 1 calculated based on Eq. 3 with $A_s = 0.08$. The aerosol influences both the cloud and surface albedo. Points are colored by N_a. Cloud fraction f_c is defined based on (a) $\tau > 1$, (b) $\tau > 2$, and (c) $\tau > 5$.

Calculations are otherwise the same as in Fig. 2. The dotted line is from (18) as described in Fig. 2. Note the shift to smaller f_c and larger A with increasing τ threshold.

Figure S2. As in Fig. S1 but for Set 2 model output. (a) is identical to Fig. 4 but is repeated here for ease of comparison.

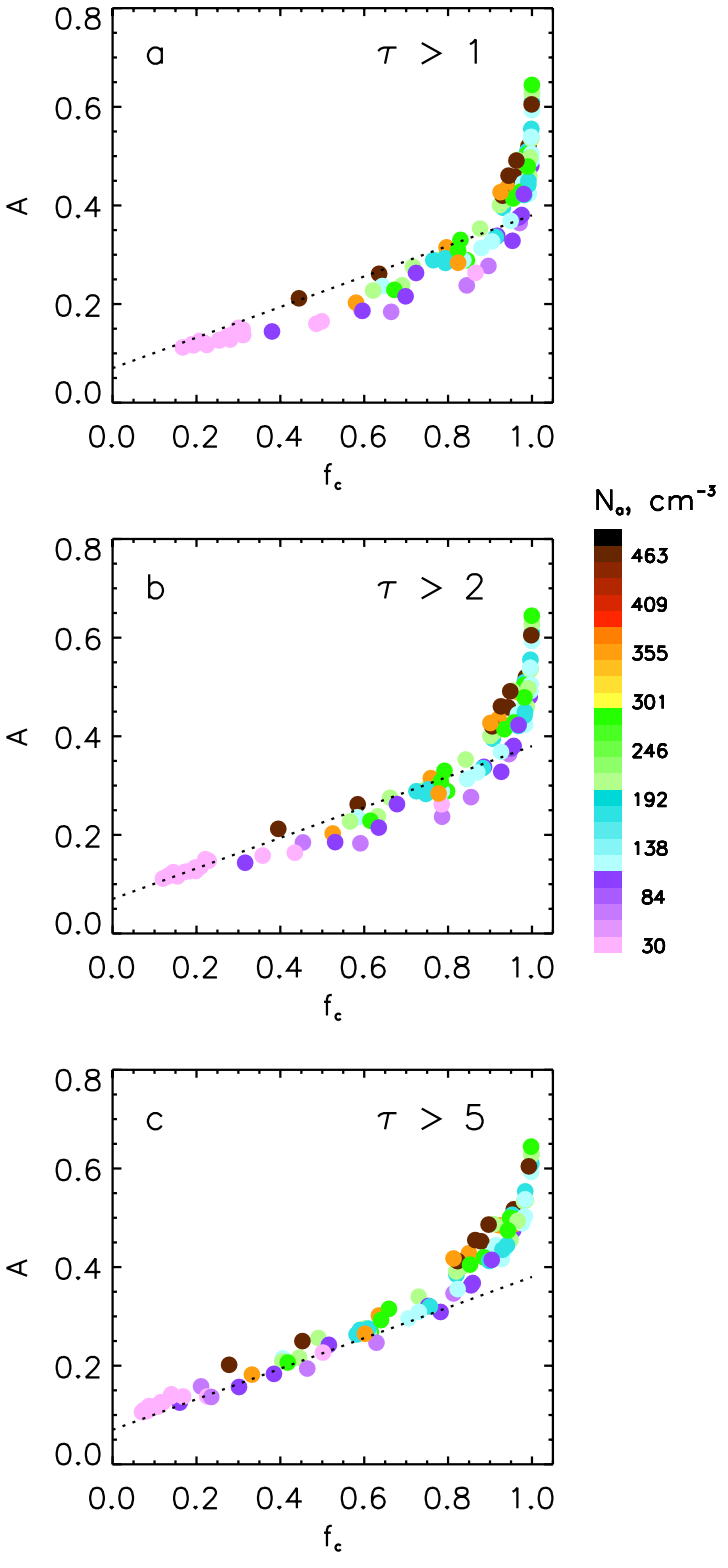
a
τ > 1
b
τ > 2
c
τ > 5
A
f_c
0.0
0.2
0.4
0.6
0.8
1.0
N_a, cm^-3
463
409
355
301
246
192
138
84
30

Fig. S1

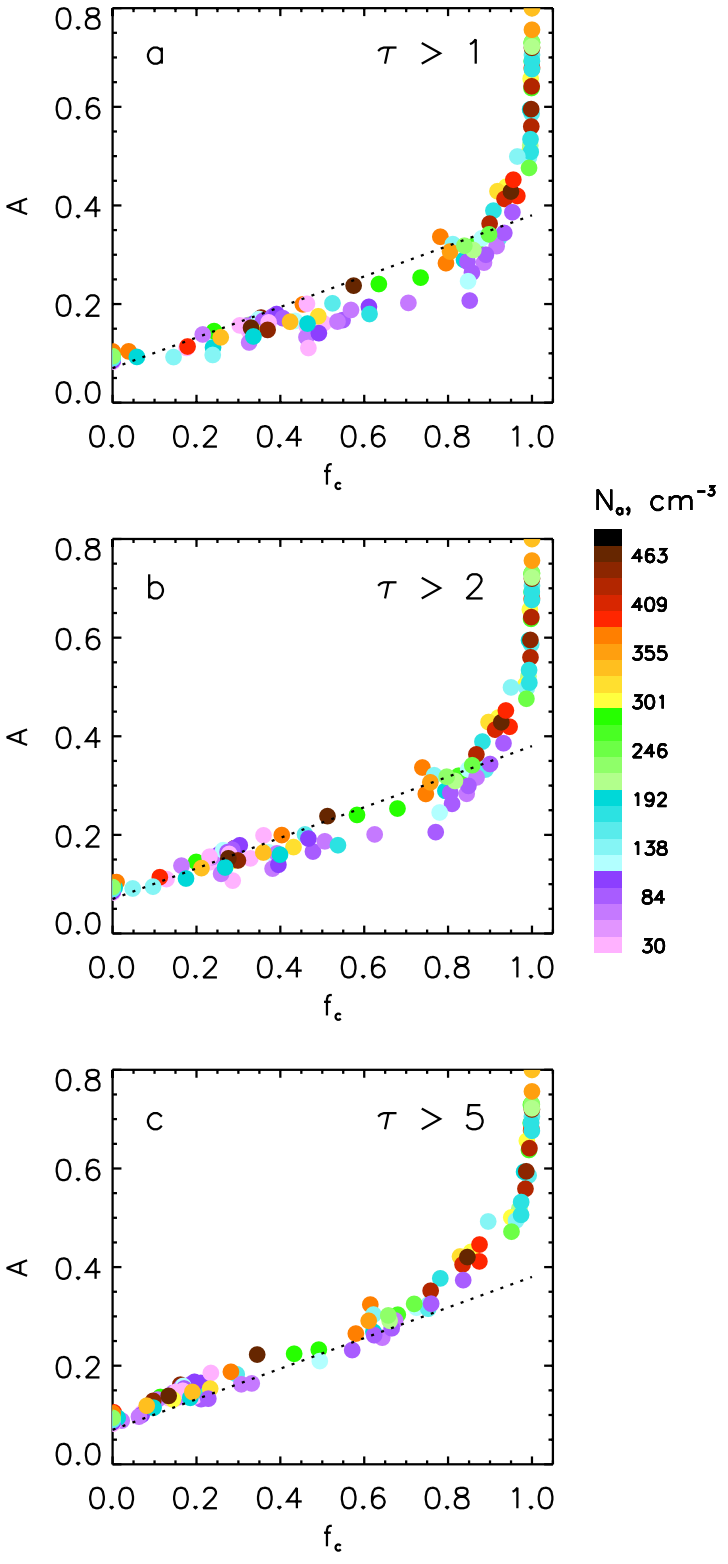
a
τ > 1
b
τ > 2
c
τ > 5
A
f_c
0.0
0.2
0.4
0.6
0.8
1.0
N_a, cm^-3
463
409
355
301
246
192
138
84
30

Fig. S2